

Full length article

## Optimizing frequency noise calibration and manipulation in an active feedback control loop

Ruixin Li <sup>a</sup>, Nanjing Jiao <sup>a</sup>, Bingnan An <sup>a</sup>, Yajun Wang <sup>a,b,\*</sup>, Wei Li <sup>a,b</sup>, Lirong Chen <sup>a,b</sup>, Long Tian <sup>a,b</sup>, Yaohui Zheng <sup>a,b</sup>

<sup>a</sup> State Key Laboratory of Quantum Optics and Quantum Optics Devices, Institute of Opto-Electronics, Shanxi University, Taiyuan 030006, China

<sup>b</sup> Collaborative Innovation Center of Extreme Optics, Shanxi University, Taiyuan, Shanxi 030006, China

### ARTICLE INFO

#### Keywords:

Signal-to-noise ratio  
Frequency noise characterization  
Frequency noise feedback

### ABSTRACT

Frequency noise is a key limitation factor for frequency sensitive ultra-high precision measurement. An excellent methodology for its calibration is the error signal extracting from a cavity length locking process via Pound–Drever–Hall (PDH) technique, and also can be applied as a noise discriminator for active feedback control. However, the stabilized laser frequency noise performance was poor to meet the applications for ultra-high precision measurement, and no literature has analyzed the cause in detail. In this Letter, we found that various of noise floors in the in-loop sensing and modulation depth in the PDH error signal should be responsible for the poor noise performance. Meanwhile, differing from the theoretical prediction (1.08), the modulation depth in frequency noise feedback controlling should be optimized by simultaneously considering the detector's gain and saturation power, cavity impedance matching, and control loop gain. In our case, it was fixed to be 0.17. The experimental results confirm our theoretical analysis well. Finally, the stabilized laser frequency noises are reduced to  $10^{-1}$  Hz/ $\sqrt{\text{Hz}}$  for out-of-loop and  $3 \times 10^{-2}$  Hz/ $\sqrt{\text{Hz}}$  for in-loop. The results demonstrate an efficient settlement solution for active frequency noise feedback control.

### 1. Introduction

A continuous wave (CW) single frequency laser with low frequency noise is a vital tool in various applications such as coherent communication [1], high-resolution spectroscopy [2], optical atomic clocks [3,4], gravitational wave detection [5], and preparing non-classical light sources [6–9]. Despite commercial laser possesses narrow linewidth and low amplitude noise, they are still confronted with high frequency noise, which cannot meet the requirements for frequency sensitive ultra-high precision measurement [10]. For example, in a high degree squeezed state generation, high frequency noise will reduce the available squeezing degree or destroy the squeezed state [11,12]. However, compared with amplitude noise, the frequency one is difficult to accurately calibrate and manipulate.

For frequency noise calibration, three routes were adopted. The first one is a beat-note method, which can more accurately calibrate the frequency noise, as low as mHz frequency band. However, compared with the laser under test, a more stable reference laser, with a similar wavelength [13] or frequency comb [14], is required. The second one is an unbalanced interferometer method [15], in which several kilometers of fiber is needed to introduce enough optical delay in one arm. The measurement frequency is limited to a lower frequency, even additional

phase-locked loop should be designed to compensate the noise introduced by the long fiber line [16]. The third frequency discriminator is a reference cavity [17], in which the frequency noise is extracted from the error signal of the Pound–Drever–Hall (PDH) technique under the cavity length locked [18]. Then, the frequency noise at Fourier frequencies within the cavity linewidth can be efficiently evaluated.

In recent years, extensive efforts for frequency noise active manipulation were executed with a reference cavity as an in-loop sensor. For a destination of gravitational wave detection (GWD), frequency noise in the range of 10 Hz–10 kHz was already reduced to  $10^{-4}$  Hz/ $\sqrt{\text{Hz}}$  level for the in-loop part [19,20]. Nevertheless, only a noise reduction level of 10 Hz/ $\sqrt{\text{Hz}}$  was observed for the out-of-loop one. In 2022, researchers in GWD groups had improved the out-of-loop noise to  $5 \times 10^{-1}$  Hz/ $\sqrt{\text{Hz}}$  with two cascaded reference cavities as the in-loop sensors [21]. They pointed out that, the in-loop dark noise and calibration technique noise of the out-of-loop, may be responsible for its poor noise performance [22]. Additionally, to realize a broadband noise performance in 10 Hz–10 kHz, all the in-loop reference cavities were installed in a vacuum system, to isolate the acoustic noise or mechanical resonances noise coupled between the acoustic resonances

\* Corresponding author.

E-mail addresses: [YJWangsxu@sxu.edu.cn](mailto:YJWangsxu@sxu.edu.cn) (Y. Wang), [yhzheng@sxu.edu.cn](mailto:yhzheng@sxu.edu.cn) (Y. Zheng).

<https://doi.org/10.1016/j.optlastec.2024.110617>

Received 21 August 2023; Received in revised form 15 November 2023; Accepted 11 January 2024

Available online 15 January 2024

0030-3992/© 2024 Elsevier Ltd. All rights reserved.

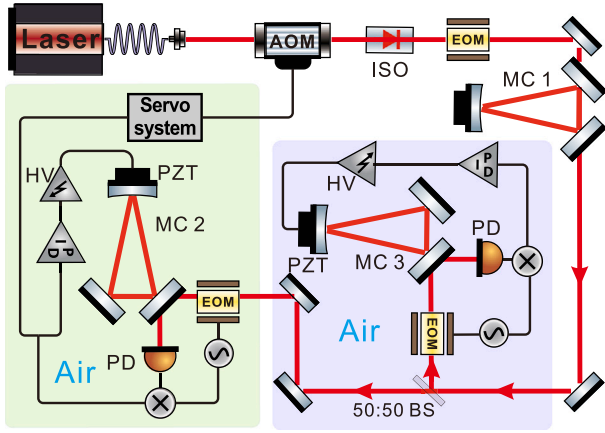


Fig. 1. Schematic setup of the frequency noise discriminator and feedback control loop. ISO, isolator; MC, mode cleaner; EOM, electro-optical modulator; BS, beam splitter; PZT, piezoelectric ceramics; HV, high voltage; PD, photo-detector; PID, proportional-integral-derivative.

of the PZT and surrounding environment. Therefore, in frequency noise active feedback control, the noise reduction is far from the shot noise level of the sensing laser, which is mainly limited by the technique noise in the control loop.

Poor frequency noise performance of the stabilized laser had been observed, but no literature has shared a detail terms of settlement solution to optimize the noise reduction level. In this Letter, we demonstrate the signal-to-noise ratio (SNR) of the in-loop frequency noise discriminator presets the upper bound for the out-of-loop noise reduction. By optimizing various of noise floors in the frequency noise discrimination and modulation depth in the PDH error signal generating processes, the SNR has been greatly improved. Whereafter, an active frequency stabilization with high SNR is constructed which stabilized the out-of-loop and in-loop noise level to  $10^{-1}$  Hz/ $\sqrt{\text{Hz}}$  and  $3 \times 10^{-2}$  Hz/ $\sqrt{\text{Hz}}$  respectively.

## 2. Experimental setup for frequency noise suppression and characterization

A frequency noise stabilization system mainly has two parts. One is the in-loop part, which contains a frequency noise discriminator, an actuator, and an electronic feedback control loop for real-time noise manipulation. The other is the out-of-loop, which is used for application. A frequency noise discriminator also is needed to accurately calibrate the noise level. Fig. 1 shows a simplified experimental configuration of the frequency noise stabilization. A NKT X15 single frequency fiber laser serves as the main laser source. Its maximum output power is 30 mW, and linewidth is less than 100 Hz. The frequency noise discriminators of the in and out-of-loops are two mode cleaners (MC) [17]. The MC is a monolithic invar ring cavity with plan mirrors and a concave mirror. The plan mirrors are directly pasted to the cavity and serve as the input and output couplers, respectively. The concave mirror, rubber O-ring and PZT assembly is clamped to the cavity to increase the tension over the PZT. This special design reduces the effect of resonances between the invar plate, PZT and mirror, and enhances the responsive bandwidth to about 100 kHz (measured by the transfer function of the PZT) [23]. A Newfocus' 2053 detector serves as an in-loop noise sensor, which unity gain saturation power and NEP are 5.6 mW and 0.34 pW/ $\sqrt{\text{Hz}}$ , respectively. Its output passes through a 3–10 MHz band-pass filter, which eliminates the excess noise over 6 MHz during the demodulating process. MC2 with a linewidth of 6.7 MHz, serves as the in-loop sensor, and is closer to perfect impedance matching. Its reflected field has less carrier power (about 2.6%), to generate a higher SNR of the PDH error signal. Then, the error signal

is divided into two parts, one is used for cavity locking, and the other is directly actuated on an AOM with 110 MHz frequency shift. MC3 with a linewidth of 2.5 MHz is used for out-of-loop frequency noise measurement. To avoid additional technique noise coupling, MC1 with a 2.5 MHz linewidth is applied to reduce the intensity noise to shot noise limit (SNL) level above 5 MHz [24]. Meanwhile, it also cleans the fundamental laser mode purity to 99.8%, which decreases high order modes induced noise to a very weak level. Meanwhile, a wedge crystal electro-optic phase modulator is arranged to provide a pure phase modulation at 8 MHz, which eliminates the etalon effect and weakens the polarization impurity induced residual amplitude modulation (RAM) noise to an extremely low level ( $2 \times 10^{-4}$  Hz/ $\sqrt{\text{Hz}}$ ) [25,26].

## 3. Theoretical model and analysis for optimizing the signal-to-noise ratio

At the outset, extensive efforts had been done to experimentally observe the relation between the stabilized noise floors of the in-loop and out-of-loop. All the evidence points out that, the stabilized laser noise is limited by the on-line noise floor in the feedback control loop. The noise floors of the frequency noise discriminator and amplitude of PDH error signal in the in-loop part should be responsible for the poor noise performance of the out-of-loop part. Here, a SNR of the in-loop is defined to analyze the noise performance of the control loop

$$SNR = S_{PDH} / S_{floor} \quad (1)$$

where,  $S_{PDH}$  is the amplitude of PDH error signal,  $S_{floor}$  is the noise floor of whole feedback control loop.

The noise floor is classified into several categories: frequency noise converted by the intensity noise on the radio frequency (RF) sideband  $S_1$ , additional optical noise from high order optical mode  $S_2$ , RAM noise  $S_3$ , loop electronic noise  $S_4$ , amplitude noise of the signal generator in demodulation  $S_5$ , shot noise of the laser  $S_6$ , and frequency noise of the reference cavity  $S_7$ . Due to the employing of MC1 and wedge crystal modulator,  $S_1$ ,  $S_2$  and  $S_3$  can be omitted in our experiment. Then, the noise floor is simplified to

$$S_{floor} = S_4 + S_5 + S_6 + S_7 \quad (2)$$

In the case of open loop, the whole noise floor of the in-loop is calibrated as the cavity far off-resonance, which sets the upper bound for out-of-loop noise reduction.  $S_5$  is monotonically increasing with the signal magnitude. Additionally, thermal noise, mechanical stability, and frequency drift of the reference MC must also be considered in low frequency band, but can be neglected above 20 kHz [27]. Shot noise is related to the incident optical power and linewidth of the MC [17]. Higher incident optical power and narrower linewidth result in a lower SNL. To enhance the SNR, the whole noise floors are minimized as much as possible. Table 1 shows the detailed noise sources in the control loop, and the maximum influence factor is the amplitude noise during the demodulation process. All the data are evaluated under open loop. As the black curve shown in Fig. 4, the total noise floor is mainly flat among the measurement frequency bandwidth (1–100 kHz), except for several noise peaks. In our experiment, frequency noises at 5 kHz are chosen to represent the noise floors in the whole bandwidth.

In frequency noise discrimination, a steeper slope of the error signal generally leads to a higher SNR [17]. Nevertheless, under the condition of modulation depth  $m \ll 1$ , the amplitude of the error signal is determined by several parameters [28]

$$S_{PDH}(f) = K P_{in} m (1 - \alpha) \frac{f / f_{pole}}{1 + (f / f_{pole})^2} \quad (3)$$

$P_{in}$  is incident laser power;  $K$  is detector electronic gain, which is also related to its saturation power. Then they co-determine the optimum modulation depth,  $m$  is modulation depth;  $\alpha = (r_1 - r_2(1 - L)) / (1 - r_1 r_2)$ , which is impedance matching factor, where  $r_1$  is the reflectivity of the cavity's input coupler mirror,  $r_2$  is the reflectivity of

**Table 1**  
Frequency noise affecting the noise floor.

Source of noise	Frequency noise (Hz/ $\sqrt{\text{Hz}}$ ) @ (5kHz)
RF sideband noise conversion $S_1$	0 (SNL)
Noise introduced by high order mode $S_2$	$2 \times 10^{-3}$ (99.8% mode matching)
Residual amplitude modulation (RAM) $S_3$	$2 \times 10^{-4}$ (Polarization purity)
Loop electronic noise $S_4$	$3 \times 10^{-3}$ (Actual measurement)
Amplitude noise of the signal generator in demodulation $S_5$	$6 \times 10^{-2}$ (Actual measurement)
MC cavity vibration $S_7$	$7 \times 10^{-3}$ (Locking instability)
MC cavity thermal noise $S_7$	$5 \times 10^{-3}$ (Material of the cavity)
Shot noise $S_6$	$3 \times 10^{-3}$ (6.7 MHz linewidth of cavity)

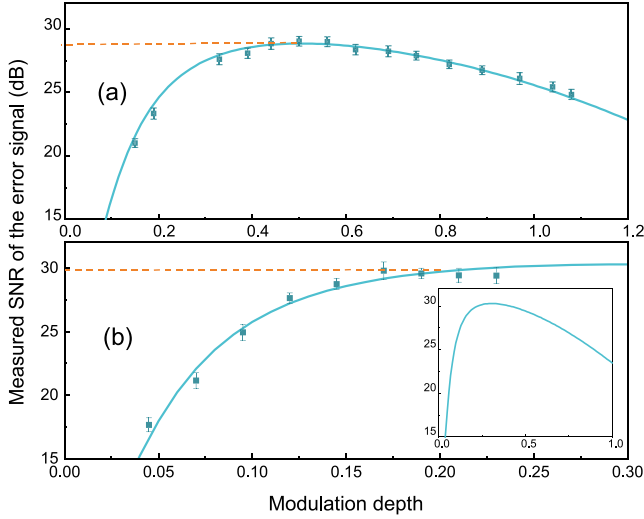


**Fig. 2.** The relationship between modulation depth and SNR of the error signal (a) with  $K = 1$  and (b)  $K = 10$ . The dotted light red line represents the best value of the SNR. The inset figure shows the whole tendency of the theoretical SNR with the modulation depth from 0 to 1.0.

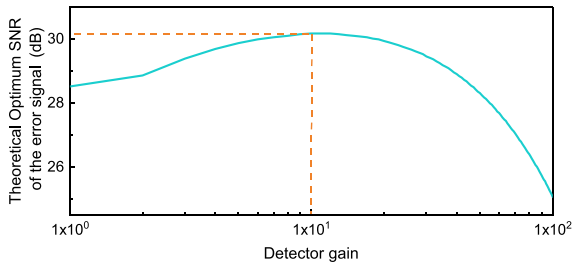


**Fig. 3.** The relationship between detection gain and SNR of the error signal.

its output coupling mirror,  $L$  is the complete round trip intracavity loss of the cavity, and  $f_{pole}$  is cavity pole. Therefore,  $S_{PDH}$  is directly proportional to  $K$ ,  $P_{in}$ ,  $m$  and impedance mismatching  $(1 - \alpha)$ . However, in frequency noise discrimination,  $m \ll 1$  is no longer valid, and  $m$  should be replaced by a Bessel function [17]. By comparing Eqs. (12)–(13) in Ref. [28] and (4.1) in Ref. [17], the SNR of the frequency discriminator of Eq. (1) is modified as [29,30]

$$SNR = \frac{2GJ_0(m)J_1(m)}{\sqrt{\frac{a}{K}J_0^2(m) + 2J_1^2(m) + 2\Omega terms + KN}} \times \frac{f/f_{pole}}{1 + (f/f_{pole})^2} \quad (4)$$

where  $G = A_{dm}/S_5$  is defined as a gain of the demodulation process, and  $A_{dm}$  is the amplitude of demodulation signal. It is confirmed to be

$G \approx 10^6$ .  $a = K\alpha$  is a coefficient related to cavity impedance matching ( $\alpha \approx 0.026$ ).  $N = S_4 + S_6 + S_7$  is additional noise of the detector for unity gain, and  $N \approx 1.3 \times 10^{-2}$  Hz/ $\sqrt{\text{Hz}}$ .  $f$  is measurement frequency,  $\Omega$  is modulation frequency,  $J_0(m)$  and  $J_1(m)$  are the 0th and 1st order Bessel function, respectively.

#### 4. Experimental results and analysis of frequency noise suppression

When the frequency noise control loop is closed, several new loop noises will be created. The noises contain the amplitude noise of the signal generator, noises transferred by reference cavity and signal wire, ambient thermal and acoustic noises, acoustic noise of PZT and so on. The in-loop noise floor is easily contaminated by these noises below 20 kHz. To mitigate these impacts, the on-line frequency noise floor measurement is chosen to be 40 kHz, and the incident laser power is 8 mW. Under feedback controlling, the in-loop noise floor determines the noise reduction level of the out-of-loop, and cannot be directly on-line measured. But it always imprints on the out-of-loop beam, which provides an efficient way for on-line observation of the in-loop noise floor. Therefore, the in-loop noise floor for different modulation depth can be confirmed by observing the out-of-loop stabilized laser noise. The SNRs are measured by the ratio between the initial noise of the laser and the stabilized laser noise under different modulation depth. For each measurement, the loop gain is optimized to the best by observing the in-loop noise floor. For different detector gain ( $K = 1, 10, 100$ ), the SNR is measured under different modulation depths, as shown in Fig. 2. For  $K = 1$  (Fig. 2(a)), SNR reaches the optimum value at  $m=0.5$  and cuts down with larger  $m$ , which is completely consistent with the theoretical one. For  $K = 10$  (Fig. 2(b)), the same tendency is forecasted by the theoretical result. However, the experimental results significantly deviate from the theoretical one after  $m=0.17$ . It is the truth that higher detector gain lowers the detector saturation power to 0.52 mW [31]. Then, the modulation depth should be cut down to avoid detector saturation. For  $K = 100$ , the measured saturation power is only 0.053 mW. The result is similar with Fig. 2(b), which is omitted. The optimized SNR for different  $K$  is also theoretically calculated as shown in Fig. 3. The maximum SNR appears around  $K = 10$ , which is also consistent with the experimental result in Fig. 2. During the experiment, all the measurements are recalibrated several times to meet an optimum SNR. Therefore,  $K = 10$  is chosen as the optimum detection gain for frequency noise feedback control.

During the optimization process of the SNR in the in-loop part, the on-line observation of the noise floor confirms the final noise reduction level. Then, the noise floors for the in-loop and out-of-loop are optimized to the best value at the optimum SNR as shown with the black curves in Fig. 4, which is less than  $10^{-1}$  Hz/ $\sqrt{\text{Hz}}$  in the measurement frequency range of 1–100 kHz. Meanwhile, with the optimum SNR, the in-loop noise is reduced by more than 40 dB around 5 kHz and reaches the best noise performance of  $3 \times 10^{-2}$  Hz/ $\sqrt{\text{Hz}}$  below 10 kHz (Fig. 4(a)). In Fig. 4(b), a noise level of  $10^{-1}$  Hz/ $\sqrt{\text{Hz}}$  for the out-of-loop is observed around 20 kHz, which is mainly limited by the total

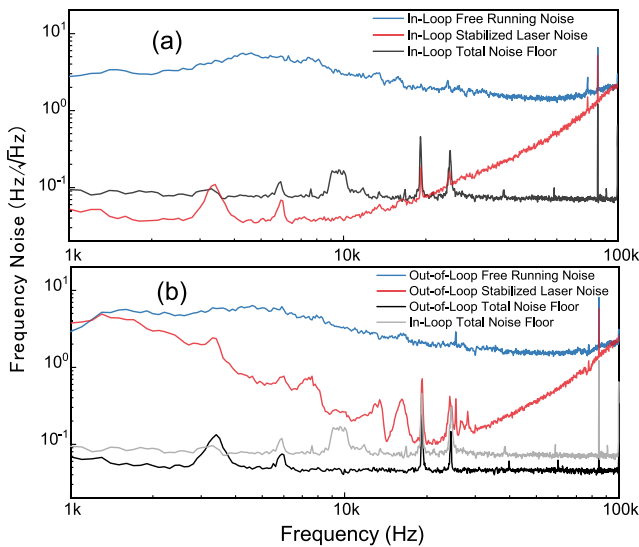


Fig. 4. Illustrates our results for (a) in-loop and (b) out-of-loop noise reduction through active feedback. Measured free running noise of laser, total noise floor and stabilized laser noise.

noise floor of the in-loop part shown in Table 1. The frequency noise rises quickly within 20 kHz and overlaps with the free-running noise below 2 kHz. Three main contributions are responsible for the high noise fluctuation in this measurement frequency range. First, several non-laser frequency noises of the in-loop part, such as amplitude noise of the signal generator, noises transferred by reference cavity and signal wire, and so on, are directly imprinted on the out-of-loop one [32]. Secondly, no thermostatic and vacuum ambiance stabilization is imported to our frequency noise discriminator, which introduces ambient thermal and acoustic noises in the frequency ranges of < 1 kHz and 1–20 kHz [23,33]. Thirdly, the cavity length is shaken by the acoustic noise of PZT below 20 kHz. This acoustic noise is mainly introduced by the electro-mechanical nature of the PZT, which is highly sensitive to acoustic resonances or the surrounding environment, including its own mount and even the optical table [23]. In our case, the mechanical resonances of the PZT can be directly observed by increasing the in-loop gain to produce a mechanical vibration of the PZT. The acoustic effect is also evidenced by the transfer function of the cavity, which the locking bandwidth of MC3 is 2 kHz, and the acoustic noise disappears after 20 kHz [34]. Furthermore, the frequency noise stabilization loop suffers from the acoustic noise seriously. Comparing the noise performances between the in-loop and out-of-loop, it can be found that the acoustic noise is limited to the frequency range of 1–20 kHz. The noise peak around 16 kHz is mainly contributed by the mechanical resonance between the cavity mirror and PZT. And the noise contribution within 1–20 kHz is mainly contributed by acoustic noise of the PZT and electronic noise of the in-loop. These influence factors cause the noise spectrum to deviate from the expected results within 20 kHz. Both in-loop and out-of-loop parts have the same noise reduction level after 20 kHz. By switching the roles of the in-loop and out-of-loop reference cavities, the same noise reductions are observed for the two loops. All the results demonstrate that the two loops exhibit uniform calibration ability without considering the three influence factors.

## 5. Conclusion

We have systematically analyzed and optimized various influence factors of the noise floor in frequency noise calibration process with a cavity. The noise floors of the in-loop and out-of-loop parts are optimized to less than  $10^{-1}$  Hz/ $\sqrt{\text{Hz}}$  in the measurement frequency range of 1–100 kHz. Incorporating with the optimized modulation depth,

the SNR of the frequency noise discriminator has greatly improved. An active frequency noise stabilization loop is constructed to reduce the frequency noise to  $10^{-1}$  Hz/ $\sqrt{\text{Hz}}$  for out-of-loop and to  $3 \times 10^{-2}$  Hz/ $\sqrt{\text{Hz}}$  for in-loop. The maximum noise reduction of out-of-loop part is mainly limited by the SNR of the in-loop part, and is contaminated by thermal and acoustic noises in circumstances and acoustic noise of the PZT. The SNR becomes the upper bound for the frequency noise active stabilization with demodulating a PDH error signal method for noise calibration. We expect that frequency noise for out-of-loop can be furtherly suppressed, by exploiting the innovative technique for total.

## Funding

Project supported by the National Key R&D Program of China (Grant No. 2020YFC2200402); National Natural Science Foundation of China (NSFC) (Grants No. 62225504, No. U22A6003, No. 62027821, No. 62375162, No. 62035015, No. 12274275, No. 12304399, No. 12174234); Key R&D Program of Shanxi, China (Grant No. 202102150101003); Program for Sanjin Scholar of Shanxi Province, China.

## CRediT authorship contribution statement

**Yajun Wang:** Conceptualization, Methodology, Software. **Yaohui Zheng:** Data curation, Writing – original draft.

## Declaration of competing interest

The authors declare the following financial interests/personal relationships which may be considered as potential competing interests: Yajun Wang reports financial support was provided by National Natural Science Foundation of China. Yaohui Zheng reports was provided by National Key Research and Development Program of China.

## Data availability

Data will be made available on request.

## References

- [1] X. Yi, S. Hu, H. Zhou, C. Tang, B. Xu, J. Zhang, K. Qiu, Phase noise effects on phase-modulated coherent optical OFDM, *IEEE Photonics J.* 8 (1) (2015) 1–8.
- [2] R. De Groote, I. Budinčević, J. Billowes, M. Bissell, T.E. Cocolios, G.J. Farooq-Smith, V. Fedosseev, K. Flanagan, S. Franchoo, R.G. Ruiz, et al., Use of a continuous wave laser and pockels cell for sensitive high-resolution collinear resonance ionization spectroscopy, *Phys. Rev. Lett.* 115 (13) (2015) 132501.
- [3] R. Le Targat, L. Lorini, Y. Le Coq, M. Zawada, J. Guéna, M. Abgrall, M. Gurov, P. Rosenbusch, D. Rovera, B. Nagórny, et al., Experimental realization of an optical second with strontium lattice clocks, *Nature Commun.* 4 (1) (2013) 2109.
- [4] B.A.C.O.N.B. Collaboration, Frequency ratio measurements at 18-digit accuracy using an optical clock network, *Nature* 591 (7851) (2021) 564–569.
- [5] M. Pitkin, S. Reid, S. Rowan, J. Hough, Gravitational wave detection by interferometry (ground and space), *Living Rev. Relativ.* 14 (2011) 1–75.
- [6] W. Yang, S. Shi, Y. Wang, W. Ma, Y. Zheng, K. Peng, Detection of stably bright squeezed light with the quantum noise reduction of 12.6 dB by mutually compensating the phase fluctuations, *Opt. Lett.* 42 (21) (2017) 4553–4556.
- [7] W. Zhang, R. Li, Y. Wang, X. Wang, L. Tian, Y. Zheng, Security analysis of continuous variable quantum key distribution based on entangled states with biased correlations, *Opt. Express* 29 (14) (2021) 22623–22635.
- [8] W. Zhang, J. Wang, Y. Zheng, Y. Wang, K. Peng, Optimization of the squeezing factor by temperature-dependent phase shift compensation in a doubly resonant optical parametric oscillator, *Appl. Phys. Lett.* 115 (17) (2019) 171103.
- [9] H. Vahlbruch, M. Mehmet, K. Danzmann, R. Schnabel, Detection of 15 dB squeezed states of light and their application for the absolute calibration of photoelectric quantum efficiency, *Phys. Rev. Lett.* 117 (11) (2016) 110801.
- [10] Y. Jiang, A. Ludlow, N.D. Lemke, R.W. Fox, J.A. Sherman, L.-S. Ma, C.W. Oates, Making optical atomic clocks more stable with 10-16-level laser stabilization, *Nat. Photonics* 5 (3) (2011) 158–161.
- [11] N. Kijbunchoo, T. McRae, D. Sigg, S. Dwyer, H. Yu, L. McCuller, L. Barsotti, C. Blair, A. Effler, M. Evans, et al., Low phase noise squeezed vacuum for future generation gravitational wave detectors, *Classical Quantum Gravity* 37 (18) (2020) 185014.

- [12] W. Zhang, N. Jiao, R. Li, L. Tian, Y. Wang, Y. Zheng, Precise control of squeezing angle to generate 11 db entangled state, *Opt. Express* 29 (15) (2021) 24315–24325.
- [13] B. Young, F. Cruz, W. Itano, J. Bergquist, Visible lasers with subhertz linewidths, *Phys. Rev. Lett.* 82 (19) (1999) 3799.
- [14] A. Cingöz, D. Yost, T. Allison, A. Ruehl, M. Fermann, I. Hartl, J. Ye, Broadband phase noise suppression in a Yb-fiber frequency comb, *Opt. Lett.* 36 (5) (2011) 743–745.
- [15] O. Llopis, P.-H. Merrer, H. Brahim, K. Saleh, P. Lacroix, Phase noise measurement of a narrow linewidth CW laser using delay line approaches, *Opt. Lett.* 36 (14) (2011) 2713–2715.
- [16] D. Li, C. Qian, Y. Li, J. Zhao, Efficient laser noise reduction method via actively stabilized optical delay line, *Opt. Express* 25 (8) (2017) 9071–9077.
- [17] E.D. Black, An introduction to Pound–Drever–Hall laser frequency stabilization, *Amer. J. Phys.* 69 (1) (2001) 79–87.
- [18] F. Schmid, J. Weitenberg, T.W. Hänsch, T. Udem, A. Ozawa, Simple phase noise measurement scheme for cavity-stabilized laser systems, *Opt. Lett.* 44 (11) (2019) 2709–2712.
- [19] C. Cahillane, G.L. Mansell, D. Sigg, Laser frequency noise in next generation gravitational-wave detectors, *Opt. Express* 29 (25) (2021) 42144–42161.
- [20] F. Meylahn, B. Wilke, Characterization of laser systems at 1550 nm wavelength for future gravitational wave detectors, *Instruments* 6 (1) (2022) 15.
- [21] F. Meylahn, N. Knust, B. Willke, Stabilized laser system at 1550 nm wavelength for future gravitational-wave detectors, *Phys. Rev. D* 105 (12) (2022) 122004.
- [22] P. Kwee, C. Bogan, K. Danzmann, M. Frede, H. Kim, P. King, J. Pöld, O. Puncken, R.L. Savage, F. Seifert, et al., Stabilized high-power laser system for the gravitational wave detector advanced LIGO, *Opt. Express* 20 (10) (2012) 10617–10634.
- [23] W.P. Bowen, Experiments Towards a Quantum Information Network with Squeezed Light and Entanglement, (Ph. D. Thesis), 2003.
- [24] N. Jiao, R. Li, Y. Wang, W. Zhang, C. Zhang, L. Tian, Y. Zheng, Laser phase noise suppression and quadratures noise intercoupling in a mode cleaner, *Opt. Laser Technol.* 154 (2022) 108303.
- [25] Z. Li, W. Ma, W. Yang, Y. Wang, Y. Zheng, Reduction of zero baseline drift of the Pound–Drever–Hall error signal with a wedged electro-optical crystal for squeezed state generation, *Opt. Lett.* 41 (14) (2016) 3331–3334.
- [26] Z. Li, Y. Tian, Y. Wang, W. Ma, Y. Zheng, Residual amplitude modulation and its mitigation in wedged electro-optic modulator, *Opt. Express* 27 (5) (2019) 7064–7071.
- [27] S. Häfner, S. Falke, C. Grebing, S. Vogt, T. Legero, M. Merimaa, C. Lisdat, U. Sterr,  $8 \times 10^{-17}$  Fractional laser frequency instability with a long room-temperature cavity, *Opt. Lett.* 40 (9) (2015) 2112–2115.
- [28] F. Bondu, O. Debieu, Accurate measurement method of Fabry-Perot cavity parameters via optical transfer function, *Appl. Opt.* 46 (14) (2007) 2611–2614.
- [29] R. Flaminio, H. Heitmann, Longitudinal control of an interferometer for the detection of gravitational waves, *Phys. Lett. A* 214 (3–4) (1996) 112–122.
- [30] F. Beauville, D. Buskulic, L. Derome, A. Dominjon, R. Flaminio, R. Hermel, F. Marion, A. Masserot, L. Massonnet, B. Mours, et al., Improvement in the shot noise of a laser interferometer gravitational wave detector by means of an output mode-cleaner, *Classical Quantum Gravity* 23 (9) (2006) 3235.
- [31] J.F. Holmes, B.J. Rask, Optimum optical local-oscillator power levels for coherent detection with photodiodes, *Appl. Opt.* 34 (6) (1995) 927–933.
- [32] T. Day, Frequency-Stabilized Solid State Lasers for Coherent Optical Communications, (Ph. D. Thesis), 1991.
- [33] K. Numata, A. Kemery, J. Camp, Thermal-noise limit in the frequency stabilization of lasers with rigid cavities, *Phys. Rev. Lett.* 93 (2004) 250602.
- [34] C.-Q. Zhang, R.-X. Li, W.-H. Zhang, N.-J. Jiao, L. Tian, Y.-J. Wang, Y.-H. Zheng, Experimental study on noise characteristics of audio frequency band in output field of optical filter cavity, *Acta Phys. Sin.* 71 (2022) 244205.